Principles of Riemannian Geometry in Neural Networks

Michael Hauser
Department of Mechanical Engineering
Pennsylvania State University
State College, PA 16801
mzh190@psu.edu

Asok Ray
Department of Mechanical Engineering
Pennsylvania State University
State College, PA 16801
axr2@psu.edu

Abstract

This study deals with neural networks in the sense of geometric transformations acting on the coordinate representation of the underlying data manifold which the data is sampled from. It forms part of an attempt to construct a formalized general theory of neural networks in the setting of Riemannian geometry. From this perspective, the following theoretical results are developed and proven for feedforward networks. First it is shown that residual neural networks are finite difference approximations to dynamical systems of first order differential equations, as opposed to ordinary networks that are static. This implies that the network is learning systems of differential equations governing the coordinate transformations that represent the data. Second it is shown that a closed form solution of the metric tensor on the underlying data manifold can be found by backpropagating the coordinate representations learned by the neural network itself. This is formulated in a formal abstract sense as a sequence of Lie group actions on the metric fibre space in the principal and associated bundles on the data manifold. Toy experiments were run to confirm parts of the proposed theory, as well as to provide intuitions as to how neural networks operate on data.

1 Introduction

The introduction is divided into two parts. Section 1.1 attempts to succinctly describe ways in which neural networks are usually understood to operate. Section 1.2 articulates a more minority perspective. It is this minority perspective that this study develops, showing that there exists a rich connection between neural networks and Riemannian geometry.

1.1 Latent variable perspectives

Neural networks are usually understood from a latent variable perspective, in the sense that successive layers are learning successive representations of the data. For example, convolution networks [10] are understood quite well as learning hierarchical representations of images [19]. Long short-term memory networks [9] are designed such that input data act on a memory cell to avoid problems with long term dependencies. More complex devices like neural Turing machines are designed with similar intuitions for reading and writing to a memory [6].

Residual networks were designed [7] with the intuition that it is easier to learn perturbations from the identity map than it is to learn an unreferenced map. Further experiments then suggest that residual networks work well because, during forward propagation and back propagation, the signal from any block can be mapped to any other block [8]. After unraveling the residual network, this attribute can be seen more clearly. From this perspective, the residual network can be understood as an ensemble of shallower networks [16].

31st Conference on Neural Information Processing Systems (NIPS 2017), Long Beach, CA, USA.

1.2 Geometric perspectives

These latent variable perspectives are a powerful tool for understanding and designing neural networks. However, they often overlook the fundamental process taking place, where successive layers successively warp the coordinate representation of the data manifold with nonlinear transformations into a form where the classes in the data manifold are linearly separable by hyperplanes. These nested compositions of affine transformations followed by nonlinear activations can be seen by work done by C. Olah (http://colah.github.io/) and published by LeCun et al. [11].

Research in language modeling has shown that the word embeddings learned by the network preserve vector offsets[12], with an example given as $x_{apples} - x_{apple} \approx x_{cars} - x_{car}$ for the word embedding vector x_i. This suggests the network is learning a word embedding space with some resemblance to group closure, with group operation vector addition. Note that closure is generally not a property of data, for if instead of word embeddings one had images of apples and cars, preservation of these vector offsets would certainly not hold at the input [3]. This is because the input images are represented in Cartesian coordinates, but are not sampled from a flat data manifold, and so one should not measure vector offsets by Euclidean distance. In Locally Linear Embedding [13], a coordinate system is learned in which Euclidean distance can be used. This work shows that neural networks are also learning a coordinate system in which the data manifold can be measured by Euclidean distance, and the coordinate representation of the metric tensor can be backpropagated through to the input so that distance can be measured in the input coordinates.

2 Mathematical notations

Einstein notation is used throughout this paper. A raised index in parenthesis, such as $x^{(l)}$, means it is the l^{th} coordinate system while $\varphi^{(l)}$ means it is the l^{th} coordinate transformation. If the index is not in parenthesis, a superscript (contravariant) free index means it is a vector, a subscript (covariant) free index means it is a covector, and a repeated index means implied summation. The . in tensors, such as $A^{a \cdot}_{\cdot b}$, are placeholders to keep track of which index comes first, second, etc.

A (topological) manifold M of dimension dim$M$ is a Hausdorff, paracompact topological space that is locally homeomorphic to $\mathbb{R}^{\text{dim}M}$ [17]. This homeomorphism $x : U \to x(U) \subseteq \mathbb{R}^{\text{dim}M}$ is called a coordinate system on $U \subseteq M$. Non-Euclidean manifolds, such as S^1, can be created by taking an image and rotating it in a circle. A feedfoward network learns coordinate transformations $\varphi^{(l)} : x^{(l)}(M) \to \left(\varphi^{(l)} \circ x^{(l)}\right)(M)$, where the new coordinates $x^{(l+1)} := \varphi^{(l)}\left(x^{(l)}\right) : M \to x^{(l+1)}(M)$, and is initialized in Cartesian coordinates $x^{(0)} : M \to x^{(0)}(M) \subseteq \mathbb{R}^{\text{dim}M}$. A data point $q \in M$ can only be represented as numbers with respect to some coordinate system; with the coordinates at layer $l+1$, q is represented as the layerwise composition $x^{(l+1)}(q) := \left(\varphi^{(l)} \circ ... \circ \varphi^{(1)} \circ \varphi^{(0)} \circ x^{(0)}\right)(q)$.

For activation function f, such as ReLU or $\tanh$, a standard feedfoward network transforms coordinates as $x^{(l+1)} := \varphi^{(l)}\left(x^{(l)}\right) := f(x^{(l)}; l)$, whereas a residual network transforms coordinates as $x^{(l+1)} := \varphi^{(l)}\left(x^{(l)}\right) := x^{(l)} + f(x^{(l)}; l)$. Note that these are global coordinates over the entire manifold. With the Softmax coordinate transformation defined as softmax $\left(x^{(L)}\right)^j := e^{W^{(L)j}x^{(L)}} / \sum_{k=1}^{K} e^{W^{(L)k}x^{(L)}}$, the probability of $q \in M$ being from class j is $P(Y = j | X = q) =$ softmax $\left(x^{(L)}(q)\right)^j$. A figure for this section is in the appendix of the full version of the paper.

3 Neural networks as $\mathcal{C}^k$ differentiable coordinate transformations

One can define entire classes of coordinate transformations. The following formulation also has the form of differentiable curves/trajectories, but because the number of dimensions often changes as one moves through the network, it is difficult to interpret a trajectory traveling through a space of changing dimensions. A standard feedforward neural network is a $\mathcal{C}^0$ function:

$$x^{(l+1)} := f(x^{(l)}; l) \tag{1}$$

A residual network has the form $x^{(l+1)} = x^{(l)} + f(x^{(l)}; l)$. However, because of eventually taking the limit as $L \to \infty$ and $l \in [0, 1] \subset \mathbb{R}$, as opposed to l being only a finitely countable index, the equivalent form of the residual network is as follows:

$$x^{(l+1)} \simeq x^{(l)} + f(x^{(l)}; l)\Delta l \tag{2}$$

where $\Delta l = 1/L$ for a uniform partition of the interval $[0, 1]$ and is implicit in the weight matrix.

One can define entire classes of coordinate transformations inspired by finite difference approximations of differential equations. These can be used to impose k^{th} order differentiable smoothness:

$$\delta x^{(l)} := x^{(l+1)} - x^{(l)} \simeq f(x^{(l)}; l)\Delta l \tag{3}$$
$$\delta^2 x^{(l)} := x^{(l+1)} - 2x^{(l)} + x^{(l-1)} \simeq f(x^{(l)}; l)\Delta l^2 \tag{4}$$

Each of these define a differential equation, but of different order smoothness on the coordinate transformations. Written in this form the residual network in Equation 3 is a first-order forward difference approximation to a $\mathcal{C}^1$ coordinate transformation and has $\mathcal{O}(\Delta l)$ error. Network architectures with higher order accuracies can be constructed, such as central differencing approximations of a $\mathcal{C}^1$ coordinate transformation to give $\mathcal{O}\left(\Delta l^2\right)$ error.

Note that the architecture of a standard feedforward neural network is a static equation, while the others are dynamic. Also note that Equation 4 can be rewritten $x^{(l+1)} = x^{(l)} + f(x^{(l)}; l)\Delta l^2 + \delta x^{(l-1)}$, where $\delta x^{(l-1)} = x^{(l)} - x^{(l-1)}$, and in this form one sees that this is a residual network with an extra term $\delta x^{(l-1)}$ acting as a sort of momentum term on the coordinate transformations. This momentum term is explored in Section 7.1.

By the definitions of the $\mathcal{C}^k$ networks given by Equations 3-4, the right hand side is both continuous and independent of Δl (after dividing), and so the limit exists as $\Delta l \to 0$. Convergence rates and error bounds of finite difference approximations can be applied to these equations. By the standard definition of the derivative, the residual network defines a system of differentiable transformations.

$$\frac{dx^{(l)}}{dl} := \lim_{\Delta l \to 0} \frac{x^{(l+\Delta l)} - x^{(l)}}{\Delta l} = f(x^{(l)}; l) \tag{5}$$
$$\frac{d^2 x^{(l)}}{dl^2} := \lim_{\Delta l \to 0} \frac{x^{(l+\Delta l)} - 2x^{(l)} + x^{(l-\Delta l)}}{\Delta l^2} = f(x^{(l)}; l) \tag{6}$$

Notations are slightly changed, by taking $l = n\Delta l$ for $n \in \{0, 1, 2, .., L-1\}$ and indexing the layers by the fractional index l instead of the integer index n. This defines a partitioning:

$$\mathcal{P} = \{0 = l(0) < l(1) < l(2) < ... < l(n) < ... < l(L) = 1\} \tag{7}$$

where $\Delta l(n) := l(n+1) - l(n)$ can in general vary with n as the $\max_n \Delta l(n)$ still goes to zero as $L \to \infty$. To reduce notational complications, this paper will write $\Delta l := \Delta l\,(n)$ for all $n \in \{0, 1, 2, ..., L-1\}$.

In [4], a deep residual convolution network was trained on ImageNet in the usual fashion except parameter weights between residual blocks at the same dimension were shared, at a cost to the accuracy of only 0.2%. This is the difference between learning an inhomogeneous first order equation $\frac{dx^{(l)}}{dl} := f(x^{(l)}; l)$ and a (piecewise) homogeneous first order equation $\frac{dx^{(l)}}{dl} := f(x^{(l)})$.

4 The Riemannian metric tensor learned by neural networks

From the perspective of differentiable geometry, as one moves through the layers of the neural network, the data manifold stays the same but the coordinate representation of the data manifold changes with each successive affine transformation and nonlinear activation. The objective of the neural network is to find a coordinate representation of the data manifold such that the classes are linearly separable by hyperplanes.

Definition 4.1. (Riemannian manifold [17]) A Riemannian manifold (M, g_{ab}) is a real smooth manifold M with an inner product, defined by the positive definite metric tensor $g_{ab} = g_{ab}(x)$, varying smoothly on the tangent space of M.

If the network has been well trained as a classifier, then by Euclidean distance two input points of the same class may be far apart when represented by the input coordinates but close together in the output coordinates. Similarly, two points of different classes may be near each other when

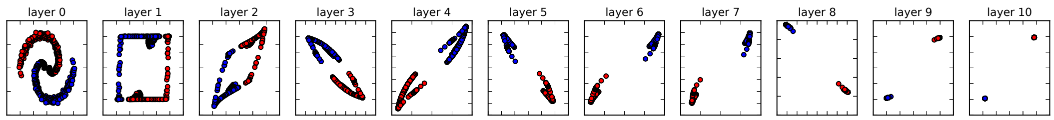

(a) A $\mathcal{C}^0$ network with sharply changing layer-wise particle trajectories.

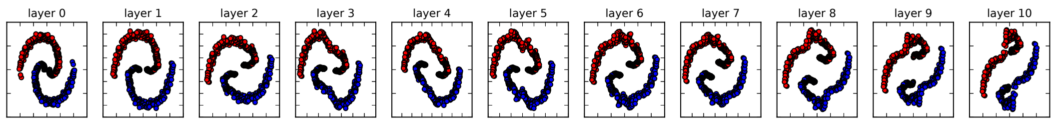

(b) A $\mathcal{C}^1$ network with smooth layer-wise particle trajectories.

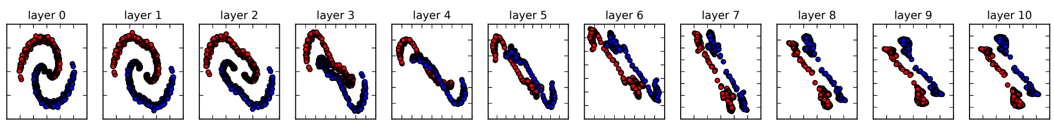

(c) A $\mathcal{C}^2$ network also exhibits smooth layer-wise particle trajectories.

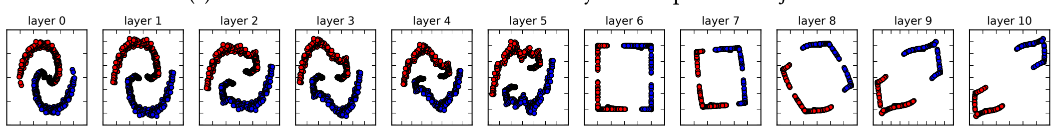

(d) A combination $\mathcal{C}^0$ and $\mathcal{C}^1$ network, where the identity connection is left out in layer 6.

Figure 1: Untangling the same spiral with 2-dimensional neural networks with different constraints on smoothness. The x and y axes are the two nodes of the neural network at a given layer l, where layer 0 is the input data. The $\mathcal{C}^0$ network is a standard network, while the $\mathcal{C}^1$ network is a residual network and the $\mathcal{C}^2$ network also exhibits smooth layerwise transformations. All networks achieve 0.0% error rates. The momentum term in the $\mathcal{C}^2$ network allows the red and blue sets to pass over each other in layers 3, 4 and 5. Figure 1d has the identity connection for all layers other than layer 6.

represented by the input coordinates but far apart in the output coordinates. These ideas form the basis of Locally Linear Embeddings [13]. The intuitive way to measure distances is in the output coordinates, which tends to be a flattened representation of the data manifold [3]. Accordingly, the metric representation in the output coordinates is defined as the standard Euclidean metric:

$$g(x^{(L)})_{a_L b_L} := \eta_{a_L b_L} \tag{8}$$

The metric tensor transforms as a tensor with coordinate transformations:

$$g(x^{(l)})_{a_l b_l} = \left(\frac{\partial x^{(l+1)}}{\partial x^{(l)}}\right)^{a_{l+1}\cdot}_{\cdot a_l} \left(\frac{\partial x^{(l+1)}}{\partial x^{(l)}}\right)^{b_{l+1}\cdot}_{\cdot b_l} g(x^{(l+1)})_{a_{l+1} b_{l+1}} \tag{9}$$

The above recursive formula is solved from the output layer to the input, i.e. the coordinate representation of the metric tensor is backpropagated through the network from output to input:

$$g(x^{(l)})_{a_l b_l} = \prod_{l'=L-1}^{l} \left[\left(\frac{\partial x^{(l'+1)}}{\partial x^{(l')}}\right)^{a_{l'+1}\cdot}_{\cdot a_{l'}} \left(\frac{\partial x^{(l'+1)}}{\partial x^{(l')}}\right)^{b_{l'+1}\cdot}_{\cdot b_{l'}} \right] \eta_{a_L b_L} \tag{10}$$

If the network is taken to be residual as in Equation 2, then the Jacobian of the coordinate transformation is found, with $\delta^{a_{l+1}\cdot}_{\cdot a_l}$ the Kronecker delta:

$$\left(\frac{\partial x^{(l+1)}}{\partial x^{(l)}}\right)^{a_{l+1}\cdot}_{\cdot a_l} = \delta^{a_{l+1}\cdot}_{\cdot a_l} + \left(\frac{\partial f\left(x^{(l)}; l\right)}{\partial x^{(l)}}\right)^{a_{l+1}\cdot}_{\cdot a_l} \Delta l \tag{11}$$

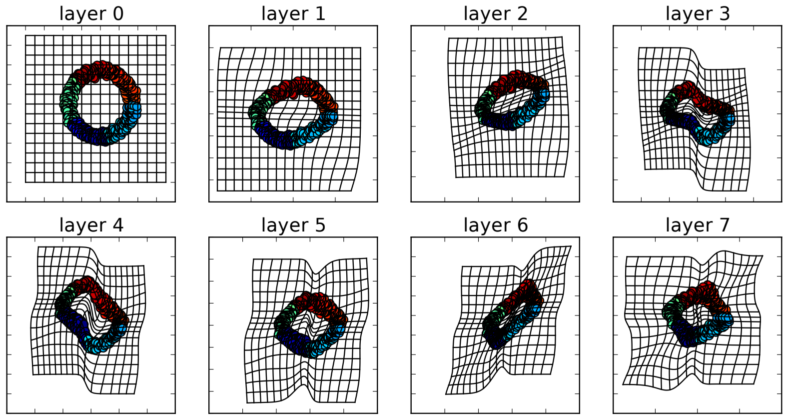

Figure 2: Layerwise coordinate transformations with a $\mathcal{C}^1$ (residual) network, used to change the shape of the input to match an output via ℓ^2 minimization. The coordinate transformations take place smoothly over the network as the next layer is a slight perturbation from the previous. Also note that if distances at the output are measured by the Euclidean metric, then to preserve the metric properties from the input, the output coordinate space becomes non Cartesian.

Backpropagating the coordinate representation of the metric tensor requires the sequence of matrix products from output to input, and can be defined for any layer l:

$$P^{a_L\cdot}_{\cdot a_l} := \prod_{l'=l}^{L-1}\left[\delta^{a_{l'+1}\cdot}_{\cdot a_{l'}} + \left(\frac{\partial f(z^{(l'+1)};l')}{\partial z^{(l'+1)}}\right)^{a_{l'+1}\cdot}_{\cdot e_{l'+1}} \left(\frac{\partial z^{(l'+1)}}{\partial x^{(l')}}\right)^{e_{l'+1}\cdot}_{\cdot a_{l'}}\Delta l\right] \tag{12}$$

where $z^{(l+1)} := W^{(l)}x^{(l)} + b^{(l)}$. With this, taking the output metric to be the standard Euclidean metric η_{ab}, the linear element can be represented in the coordinate space for any layer l:

$$ds^2 = P^{a\cdot}_{\cdot a_l} P^{b\cdot}_{\cdot b_l}\eta_{ab}dx^{a_l}dx^{b_l} \tag{13}$$

The data manifold is independent of coordinate representation. At the output where distances are measured by the standard Euclidean metric an ϵ-ball can be defined. The linear element in Equation 13 defines the corresponding δ-ball at layer l. This can be used to see what in the input space the neural network says is close in the output space.

As $L \to \infty$ this becomes an infinite product of matricies (from our infinite applications of the chain rule). Analogous to the scalar case, $P^{a_L\cdot}_{\cdot a_0} = \prod_{l'=0}^{L-1}(\delta^{a_{l'+1}\cdot}_{\cdot a_{l'}} + A^{a_{l'+1}\cdot}_{\cdot a_{l'}})$ converges if $\sum_{l'=0}^{L-1}||A^{a_{l'+1}\cdot}_{\cdot a_{l'}}||_2$ converges [18]. For a fully connected network with activation $\tanh(z)$, the following inequality holds:

$$\sum_{l'=0}^{L-1}||A^{a_{l'+1}\cdot}_{\cdot a_{l'}}||_2 = \sum_{l'=0}^{L-1}||\left(\frac{\partial f(z^{(l'+1)};l')}{\partial z^{(l'+1)}}\right)^{a_{l'+1}\cdot}_{\cdot e_{l'+1}} \left(\frac{\partial z^{(l'+1)}}{\partial x^{(l')}}\right)^{e_{l'+1}\cdot}_{\cdot a_{l'}}\Delta l||_2 \leq$$
$$\sum_{l'=0}^{L-1} 2\cdot ||W^{e_{l'+1}\cdot}_{\cdot a_{l'}}||_2 \Delta l = 2\cdot E\left[||W^{e_{l'+1}\cdot}_{\cdot a_{l'}}||_2\right] < \infty \tag{14}$$

where $||.||_2$ is the ℓ^2 norm and $E[.]$ is the expectation. This shows that the infinite sum converges, implying that in the limit Equation 12 converges. In the limit the actions of the coordinate transformations on the metric tensor smoothly transform the metric tensor coordinate representation.

This analysis has so far assumed a constant layerwise dimension, which is not how most neural networks are used in practice, where the number of nodes often changes. This is handled by considering the pullback metric [17].

Definition 4.2. (Pushforward map) Let M and N be topological manifolds, $\varphi^{(l)} : M \to N$ a smooth map and TM and TN be their respective tangent spaces. Also let $X \in TM$ where $X : \mathcal{C}^{\infty}(M) \to \mathbb{R}$, and $f \in \mathcal{C}^{\infty}(N)$. The pushfoward map $\varphi_*^{(l)} : TM \to TN$ takes an element $X \to \varphi_*^{(l)} X$ and is defined by its action on f as $\left(\varphi_*^{(l)} X\right)(f) := X\left(f \circ \varphi^{(l)}\right)$.

Definition 4.3. (Pullback metric) Let (M, g_M) and (N, g_N) be Riemannian manifolds, $\varphi^{(l)} : M \to N$ a smooth map and $\varphi_*^{(l)} : TM \to TN$ the pushfoward between their tangent spaces TM and TN. Then the pullback metric on M is given by $g_M(X, Y) := g_N\left(\varphi_*^{(l)} X, \varphi_*^{(l)} Y\right) \forall X, Y \in TM$.

In practice being able to change dimensions in the neural network is important for many reasons. One reason is that neural networks usually have access to a limited number of types of nonlinear coordinate transformations, for example $\tanh$, σ and ReLU. This severly limits the ability of the network to separate the wide variety of manifolds that exist. For example, the networks have difficulty linearly separating the simple toy spirals in Figures 1 because they only have access to coordinate transformations of the form $\tanh$. If instead they had access to a coordinate system that was more appropriate for spirals, such as polar coordinates, they could very easily separate the data. This is the reason why Locally Linear Embeddings [13] could very easily discover the coordinate charts for the underlying manifold, because k-nearest neighbors is an extremely flexible type of nonlinearity. Allowing the network to go into higher dimensions makes it easier to separate data.

5 Lie Group actions on the metric fibre bundle

This section will abstractly formulate Section 4 as neural networks learning sequences of left Lie Group actions on the metric (fibre) space over the data manifold to make the metric representation of the underlying data manifold Euclidean. Several definitions, which can be found in the appendix in the full version of this paper, are needed to formulate Lie group actions on principal and associated fibre bundles, namely of bundles, fibre bundles, Lie Groups and their actions on manifolds [17].

Definition 5.1. (Principal fibre bundle) A bundle (E, π, M) is called a principal G-bundle if:

(i.) E is equipped with a right G-action $\triangleleft$

(ii.) The right G-action $\triangleleft$ is free.

(iii.) (E, π, M) is (bundle) isomorphic to $(E, \rho, E/G)$ where the surjective projection map $\rho : E \to E/G$ is defined by $\rho(\epsilon) := [\epsilon]$ as the equivalence class of points of ϵ

Remark. (Principal bundle) The principal fibre bundle can be thought of (locally) as a fibre bundle with fibres G over the base manifold M.

Definition 5.2. (Associated fibre bundle) Given a G principal bundle and a smooth manifold F on which exists a left G-action $\triangleright: G \times F \to F$, the associated fibre bundle (P_F, π_F, M) is defined as follows:

(i.) let $\sim_G$ be the relation on $P \times F$ defined as follows:

$(p, f) \sim_G (p', f') :\iff \exists h \in G : p' = p \triangleleft h$ and $f' = h^{-1} \triangleright f$, and thus $P_F := (P \times F) / \sim_G$.

(ii.) define $\pi_F : P_F \to M$ by $\pi_F([(p, f)]) := \pi(p)$

Neural network actions on the manifold M are a (layerwise) sequence of left G-actions on the associated (metric space) fibre bundle. Let the dimension of the manifold $d := \dim M$.

The group G is taken to be the general linear group of dimension d over $\mathbb{R}$, i.e. $G = GL(d, \mathbb{R}) := \{\phi : \mathbb{R}^d \to \mathbb{R}^d | \det \phi \neq 0\}$.

The principal bundle P is taken to be the frame bundle, i.e. $P = LM := \cup_{p \in M} L_p M := \cup_{p \in M} \{(e_1, ..., e_d) \in T_p M | (e_1, ..., e_d) \text{ is a basis of } T_p M\}$, where $T_p M$ is the tangent space of M at the point $p \in M$.

The right G-action $\triangleleft$: $LM \times GL(d, \mathbb{R}) \to LM$ is defined by $e \triangleleft h = (e_1, ..., e_d) \triangleleft h := (h^{a_l \cdot}_{.1} e_{a_l}, ..., h^{a_l \cdot}_{.d} e_{a_l})$, which is the standard transformation law of linear algebra.

The fibre F in the associated bundle will be the metric tensor space, with two lower indicies, and so $F = \left(\mathbb{R}^d\right)^* \times \left(\mathbb{R}^d\right)^*$, where the $*$ denotes the cospace. With this, the left G-action $\triangleright$: $GL(d, \mathbb{R}) \times F \to F$ is defined by $\left(h^{-1} \triangleright g\right)_{a_l b_l} := g_{a_{l+1} b_{l+1}} h^{a_{l+1} \cdot}_{.a_l} h^{b_{l+1} \cdot}_{.b_l}$

Layerwise sequential applications of the left G-action from output to input is thus simply understood:

$$\left(h_0^{-1} \triangleright h_1^{-1} \triangleright \ldots \triangleright h_L^{-1} \triangleright g\right)_{a_0 b_0} = \left(h_0^{-1} \bullet \ldots \bullet h_L^{-1}\right) \triangleright g_{a_L b_L} = \prod_{l'=0}^{L-1} \left(h^{a_{l'+1}\cdot}_{\cdot a'_l} h^{b_{l'+1}\cdot}_{\cdot b_{l'}}\right) g_{a_L b_L} \tag{15}$$

This is equivalent to Equation 10, only formulated in a formal, abstract sense.

6 Backpropagation as a sequence of right Lie Group actions

A similar analysis that has been performed in Sections 4 and 5 can be done to generalize error backpropagation as a sequence of left Lie Group actions on the output error, as well as show that backpropagation converges as $L \to \infty$. The discrete layerwise error backpropagation algorithm [14] is derived using the chain rule on graphs. The closed form solution of the gradient of the output error E with respect to any layer weight $W^{(l-1)}$ can be solved for recursively from the output, by backpropagating errors:

$$\frac{\partial E}{\partial W^{(l-1)}} = \left(\frac{\partial E}{\partial x^{(L)}}\right)_{a_L} \prod_{l'=l}^{L-1} \left(\frac{\partial x^{(l'+1)}}{\partial x^{(l')}}\right)^{a_{l'+1}\cdot}_{\cdot a_{l'}} \left(\frac{\partial x^{(l)}}{\partial W^{(l-1)}}\right)^{a_l} \tag{16}$$

In practice, one further applies the chain rule $\left(\frac{\partial x^{(l)}}{\partial W^{(l-1)}}\right)^{a_{l'}} = \left(\frac{\partial x^{(l)}}{\partial z^{(l)}}\right)^{a_l\cdot}_{\cdot b_l} \left(\frac{\partial z^{(l)}}{\partial W^{(l-1)}}\right)^{b_l}$. Note that $W^{(l-1)}$ is a coordinate chart on the parameter manifold [1], *not* the data manifold.

In this form it is immediately seen that error backpropagation is a sequence of right G-actions $\prod_{l'=l}^{L-1} \left(\frac{\partial x^{(l'+1)}}{\partial x^{(l')}}\right)^{a_{l'+1}\cdot}_{\cdot a_{l'}}$ on the output frame bundle $\left(\frac{\partial}{\partial x^{(L)}}\right)_{a_L}$. This transforms the frame bundle acting on E to the coordinate system at layer l, and thus puts it in the same space as $\left(\frac{\partial x^{(l)}}{\partial W^{(l-1)}}\right)^{a_l}$.

For the residual network, the transformation matrix Equation 11 can be inserted into Equation 16.By the same logic as Equation 14, the infinite tensor product in Equation 16 converges in the limit $L \to \infty$ in the same way as in Equation 12, and so it is not rewritten here. In the limit this becomes a smooth right G-action on the frame bundle, which itself is acting on the error cost function.

7 Numerical experiments

This section presents the results of numerical experiments used to understand the proposed theory. The $\mathcal{C}^\infty$ hyperbolic tangent has been used for all experiments, with weights initialized according to [5]. For all of the experiments, layer 0 is the input Cartesian coordinate representation of the data manifold, and the final layer L is the last hidden layer before the linear softmax classifier. GPU implementations of the neural networks are written in the Python library Theano [2, 15].

7.1 Neural networks with $\mathcal{C}^k$ differentiable coordinate transformations

As described in Section 3, k^{th} order smoothness can be imposed on the network by considering network structures defined by e.g. Equations 3-4. As seen in Figure 1a, the standard $\mathcal{C}^0$ network with no impositions on differentiability has very sharp layerwise transformations and separates the data in an unintuitive way. The $\mathcal{C}^1$ residual network and $\mathcal{C}^2$ network can be seen in Figures 1b and 1c, and exhibit smooth layerwise transformations and separate the data in a more intuitive way. Forward differencing is used for the $\mathcal{C}^1$ network, while central differencing was used for the $\mathcal{C}^2$ network, except at the output layer where backward differencing was used, and at the input first order smoothness was used as forward differencing violates causality.

In Figure 1c one can see that for the $\mathcal{C}^2$ network the red and blue data sets pass over each other in layers 4, 5 and 6. This can be understood as the $\mathcal{C}^2$ network has the same form as a residual network, with an additional momentum term pushing the data past each other.

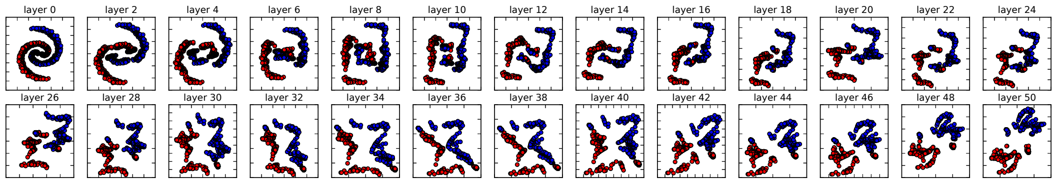

(a) A batch size of 300 for untangling data. As early as layer 4 the input connected sets have been disconnected and the data are untangled in an unintuitive way. This means a more complex coordinate representation of the data manifold was learned.

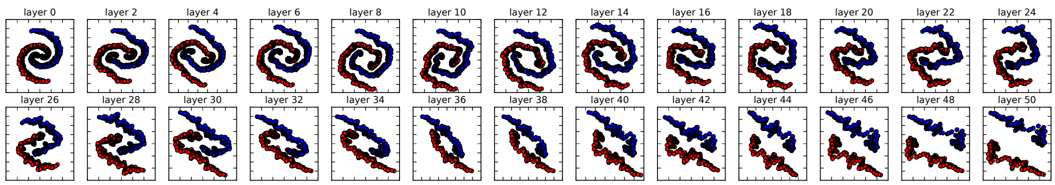

(b) A batch size of 1000 for untangling data. Because the large batch size can well-sample the data manifold, the sprial sets stay connected and are untangled in an intuitive way. This means a simple coordinate representation of the data manifold was learned.

Figure 3: The effect of batch size on coordinate representation learned by the same 2-dimensional $\mathcal{C}^1$ network, where layer 0 is the input representation, and both examples achieve 0% error. A basic theorem in topology says continuous functions map connected sets to connected sets. A small batch size of 300 during training sparsely samples from the connected manifold and the network learns overfitted coordinate representations. With a larger batch size of 1000 during training the network learns a simpler coordinate representation and keeps the connected input connected throughout.

7.2 Coordinate representations of the data manifold

As described in Sections 4 and 5, the network is learning a sequence of coordinate transformations, beginning with Cartesian coordinates, to find a coordinate representation of the data manifold that is required by the cost function. This process can be visualized in Figure 2. This experiment used a $\mathcal{C}^1$ network with an ℓ^2 minimization between the input and output data, so the group actions on the principal and associated bundles act smoothly along the fibres. Grid lines were not displayed in the other experiments so the specific effects of the other experiments can be more clearly seen.

In the forward direction, beginning with Cartesian coordinates, a sequence of $\mathcal{C}^1$ differential coordinate transformations is applied to find a nonlinear coordinate representation of the data manifold such that in the output coordinates the classes satisfy the cost restraint. In the reverse direction, starting with a standard Euclidean metric at the output Equation 8, the coordinate representation of the metric tensor is backpropagated through the network to the input by Equations 9-10 to find the metric tensor representation in the input Cartesian coordinates.

7.3 Effect of batch size on set connectedness and topology

A basic theorem in topology says that continuous functions map connected sets to connected sets. However, in Figure 3a it is seen that as early as layer 4 the continuous neural network is breaking the connected input set into disconnected sets. Additionally, and although it achieves 0% error, it is learning very complicated and unintuitive coordinate transformations to represent the data in a linearly separable form. This is because during training with a small batch size of 300 in the stochastic gradient descent search, the underlying manifold was not sufficiently sampled to represent the entire connected manifold and so it seemed disconnected.

This is compared to Figure 3b in which a larger batch size of 1000 was used and was sufficiently sampled to represent the entire connected manifold, and the network was also able to achieve 0% error. The coordinate transformations learned by the neural network with the larger batch size seem to more intuitively untangle the data in a simpler way than that of Figure 3a. Note that this experiment is in 2-dimensions, and with higher dimensional data the issue of batch size and set connectedness becomes exponentially more important.

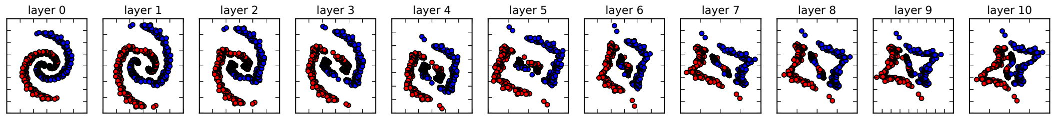

(a) A 10 layer $\mathcal{C}^1$ network struggles to separate the spirals and has 1% error rate.

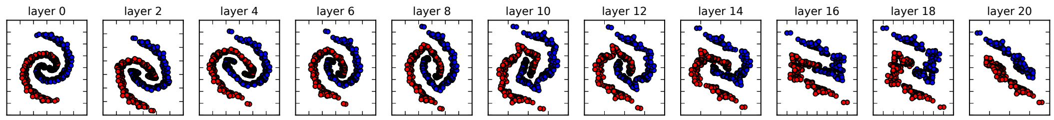

(b) A 20 layer $\mathcal{C}^1$ network is able to separate the spirals and has 0% error rate.

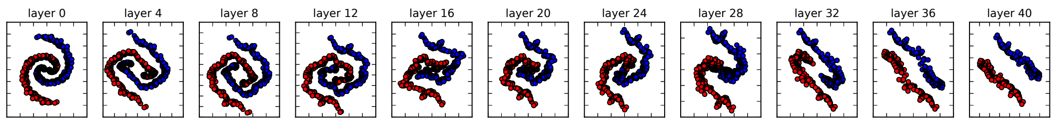

(c) A 40 layer $\mathcal{C}^1$ network is able to separate the spirals and has 0% error rate.

Figure 4: The effect of number of layers on the separation process of a $\mathcal{C}^1$ neural network. In Figure 4a it is seen that the Δl is too large to properly separate the data. In Figures 4b and 4c the Δl is sufficiently small to separate the data. Interestingly, the separation process is not as simple as merely doubling the parameterization and halving the partitioning in Equation 7 because this is a nonlinear system of ODE's. This is seen in Figures 4b and 4c; the data are at different levels of separation at the same position of layer parameterization, for example by comparing layer 18 in Figure 4b to layer 36 in Figure 4c.

7.4 Effect of number of layers on the separation process

This section compares the process in which 2-dimensional $\mathcal{C}^1$ networks with 10, 20 and 40 layers separate the same data, thus experimenting on the Δl in the partitioning of Equation 7, as seen in Figure 4. The 10 layer network is unable to properly separate the data and achieves a 1% error rate, whereas the 20 and 40 layer networks both achieve 0% error rates. In Figures 4b and 4c it is seen that at same positions of layer parameterization, for example layers 18 and 36 respectively, the data are at different levels of separation. This implies that the partitioning cannot be interpreted as simply as halving the Δl when doubling the number of layers. This is because the system of ODE's are nonlinear and the Δl is implicit in the weight matrix.

8 Conclusions

This paper forms part of an attempt to construct a formalized general theory of neural networks as a branch of Riemannian geometry. In the forward direction, and starting in Cartesian coordinates, the network is learning a sequence of coordinate transformations to find a coordinate representation of the data manifold that is linearly separable. This implicitly imposes a flatness constraint on the metric tensor in this learned coordinate system. One can then backpropagate the coordinate representation of the metric tensor to find its form in Cartesian coordinates. This can be used to define an $\epsilon - \delta$ relationship between the input and output data. Coordinate backpropagation was formulated in a formal, abstract sense in terms of Lie Group actions on the metric fibre bundle. The error backpropagation algorithm was then formulated in terms of Lie group actions on the frame bundle. For a residual network in the limit, the Lie group acts smoothly along the fibres of the bundles. Experiments were conducted to confirm and better understand aspects of this formulation.

9 Acknowledgements

This work has been supported in part by the U.S. Air Force Office of Scientific Research (AFOSR) under Grant No. FA9550-15-1-0400. The first author has been supported by PSU/ARL Walker Fellowship. Any opinions, findings and conclusions or recommendations expressed in this publication are those of the authors and do not necessarily reflect the views of the sponsoring agencies.

References

[1] Shun-ichi Amari and Hiroshi Nagaoka. *Methods of information geometry*, volume 191. American Mathematical Soc., 2007.

[2] Frédéric Bastien, Pascal Lamblin, Razvan Pascanu, James Bergstra, Ian Goodfellow, Arnaud Bergeron, Nicolas Bouchard, David Warde-Farley, and Yoshua Bengio. Theano: new features and speed improvements. *arXiv preprint arXiv:1211.5590*, 2012.

[3] Yoshua Bengio, Grégoire Mesnil, Yann Dauphin, and Salah Rifai. Better mixing via deep representations. In *Proceedings of the 30th International Conference on Machine Learning (ICML-13)*, pages 552–560, 2013.

[4] Alexandre Boulch. Sharesnet: reducing residual network parameter number by sharing weights. *arXiv preprint arXiv:1702.08782*, 2017.

[5] Xavier Glorot and Yoshua Bengio. Understanding the difficulty of training deep feedforward neural networks. In *Aistats*, volume 9, pages 249–256, 2010.

[6] Alex Graves, Greg Wayne, and Ivo Danihelka. Neural turing machines. *arXiv preprint arXiv:1410.5401*, 2014.

[7] Kaiming He, Xiangyu Zhang, Shaoqing Ren, and Jian Sun. Deep residual learning for image recognition. In *Proceedings of the IEEE Conference on Computer Vision and Pattern Recognition*, pages 770–778, 2016.

[8] Kaiming He, Xiangyu Zhang, Shaoqing Ren, and Jian Sun. Identity mappings in deep residual networks. In *European Conference on Computer Vision*, pages 630–645. Springer, 2016.

[9] Sepp Hochreiter and Jürgen Schmidhuber. Long short-term memory. *Neural computation*, 9(8):1735–1780, 1997.

[10] Alex Krizhevsky, Ilya Sutskever, and Geoffrey E Hinton. Imagenet classification with deep convolutional neural networks. In *Advances in neural information processing systems*, pages 1097–1105, 2012.

[11] Yann LeCun, Yoshua Bengio, and Geoffrey Hinton. Deep learning. *Nature*, 521(7553):436–444, 2015.

[12] Tomas Mikolov, Wen-tau Yih, and Geoffrey Zweig. Linguistic regularities in continuous space word representations. In *Hlt-naacl*, volume 13, pages 746–751, 2013.

[13] Sam T Roweis and Lawrence K Saul. Nonlinear dimensionality reduction by locally linear embedding. *science*, 290(5500):2323–2326, 2000.

[14] David E Rumelhart, Geoffrey E Hinton, and Ronald J Williams. Learning internal representations by error propagation. Technical report, DTIC Document, 1985.

[15] Theano Development Team. Theano: A Python framework for fast computation of mathematical expressions. *arXiv e-prints*, abs/1605.02688, May 2016.

[16] Andreas Veit, Michael J Wilber, and Serge Belongie. Residual networks behave like ensembles of relatively shallow networks. In *Advances in Neural Information Processing Systems*, pages 550–558, 2016.

[17] Gerard Walschap. *Metric structures in differential geometry*, volume 224. Springer Science & Business Media, 2012.

[18] Joseph Henry Maclagan Wedderburn. *Lectures on matrices*, volume 17. American Mathematical Soc., 1934.

[19] Matthew D Zeiler, Dilip Krishnan, Graham W Taylor, and Rob Fergus. Deconvolutional networks. In *Computer Vision and Pattern Recognition (CVPR), 2010 IEEE Conference on*, pages 2528–2535. IEEE, 2010.